# DFT-based ab initio study of the electronic and optical properties of cesium based fluoro-perovskite CsMF3 (M=Ca and Sr)

**Article** *in* International Journal of Modern Physics B · December 2012

Impact Factor: 0.94 · DOI: 10.1142/S0217979212501998



**10 authors**, including:

Rabah Khenata
Mascara Universit
**355** PUBLICATIONS **2,209** CITATIONS

SEE PROFILE

Abbar Boucif
University of Sidi-Bel-Abbes
**72** PUBLICATIONS **749** CITATIONS

SEE PROFILE

International Journal of Modern Physics B
Vol. 26, No. 32 (2012) 1250199 (13 pages)

DOI: 10.1142/S0217979212501998





# DFT-BASED *AB INITIO* STUDY OF THE ELECTRONIC AND OPTICAL PROPERTIES OF CESIUM BASED FLUORO-PEROVSKITE $CsMF_3$ (M = Ca AND Sr)

M. HARMEL*, H. KHACHAI*,†, M. AMERI*, R. KHENATA*,‡, N. BAKI*,
A. HADDOU*,†, B. ABBAR§, Ş. UĞUR¶, S. BIN OMRAN‖ and F. SOYALP**

*Physics Department, Djillali Liabes University of Sidi Bel-Abbes, Algeria
†Applied Materials Laboratory, Electronics Department
Djillali Liabes University of Sidi Bel-Abbes, Algeria
‡Laboratoire de Physique Quantique et de Modélisation Mathématique de la matière (LPQ3M),
Université de Mascara, 29000 Mascara, Algeria
§Modeling and Simulation in Materials Science Laboratory, Physics Department,
Djillali Liabès University of Sidi Bel-Abbès, Sidi Bel-Abbès 22000, Algeria
¶Department of Physics, Faculty of Sciences, Gazi University, Turkey
‖Department of Physics and Astronomy, Faculty of Science, King Saud University,
P. O. Box 2455, Riyadh 11451, Saudi Arabia
**Department of Physics, Faculty of Education, Yüzüncü Yıl University,
65080, Van, Turkey
‡khenata_rabah@yahoo.fr

Received 31 August 2012
Revised 29 September 2012
Accepted 14 October 2012
Published 15 November 2012

Density functional theory (DFT) is performed to study the structural, electronic and optical properties of cubic fluoroperovskite $AMF_3$ (A = Cs; M = Ca and Sr) compounds. The calculations are based on the total-energy calculations within the full-potential linearized augmented plane wave (FP-LAPW) method. The exchange-correlation potential is treated by local density approximation (LDA) and generalized gradient approximation (GGA). The structural properties, including lattice constants, bulk modulus and their pressure derivatives are in very good agreement with the available experimental and theoretical data. The calculations of the electronic band structure, density of states and charge density reveal that compounds are both ionic insulators. The optical properties (namely: the real and the imaginary parts of the dielectric function $\varepsilon(\omega)$, the refractive index $n(\omega)$ and the extinction coefficient $k(\omega)$) were calculated for radiation up to 40.0 eV.

*Keywords*: DFT; fluoroperovskite; electronic structure; optical properties.

‡Corresponding author.

## 1. Introduction

Perovskite structure with the general chemical form $AMX_3$ is one of the most commonly occurring and important in all of materials science. Perovskite has revived great interests from academia and industry due to their extended physical properties, such as superconductivity, colossal magnetoresistance, ionic conductivity, and a multitude of dielectric properties, which are of great importance in microelectronics and telecommunication.[1] Furthermore, these compounds are interesting for dielectric studies and most of them find application in optical, electronic and other solid-state devices. In fact, the optical properties of perovskites compounds are anisotropic and show the phenomenon of birefringence and their geometry is related to the chemical composition, temperature and pressure.[2] According to Lufaso and Woodward[3] the cubic perovskites can transform into other crystal structures. The herein studied perovskites does not exhibit structural phase transition at low temperature.

Ternary fluorides with the perovskite crystal structure are selected for this study, have been extensively studied over several decades, as they have several potential applications because of their optical properties[4,5] high-temperature super-ionic behavior,[6] and physical properties, such as ferroelectricity,[7] antiferromagnetism[8] and semiconductivity.[9] In particular, $CsMF_3$ (M = Ca, Sr) are luminescent materials and could be used for elaboration of color television screen.

Moreover, the fluoroperovskite compounds can be used in the medical field to measure the dose during radiation therapy, and they may also used in the manufacture of radiation imaging plates for X-rays, gamma-rays and thermal neutrons for medical and nondestructive testing applications.

In this paper, we investigate the structural, electronic and optical properties of fluoroperovskite structures ($CsCaF_3$ and $CsSrF_3$) using a full potential linearized augmented plane wave method (FP-LAPW) in the framework of density functional theory (DFT) with both local density approximation (LDA) and generalized gradient approximations (GGA) for exchange and correlation potential. The organization of this paper is as follows: The computational method we have adopted for the calculations is described in Sec. 2. The most relevant results obtained for the structural, electronic and optical properties are presented and discussed in Sec. 3. Finally, in Sec. 4, we summarize the main conclusions of our work.

## 2. Method of Calculations

The present calculations were done with the FP-LAPW method[10] to solve the Kohn Sham equations as implemented in the WIEN2K code.[11] This method based on DFT[12] has proven to be one of the most accurate methods for the computation of the electronic structure of solids.[13,14] The exchange-correlation potential was described within the LDA of Perdew and Wang (LDA-PW)[15] and the GGA of Perdew–Burke–Ernzerhof (GGA-PBE).[16] In the FP-LAPW method, the wavefunction, charge density and potential are expanded by spherical harmonic

functions inside nonoverlapping spheres surrounding the atomic sites (muffin-tin spheres) and by a plane waves basis set in the remaining space of the unit cell (interstitial region). The plane wave cutoff of $K_{\max} = 8.0/R_{\mathrm{MT}}$ ($R_{\mathrm{MT}}$ is the smallest muffin-tin radius) is chosen for the expansion of the wavefunctions in the interstitial region while the charge density is Fourier expanded up to $G_{\max} = 14$ Bohr$^{-1}$. The muffin-tin radius was assumed to be 2.5 u.a and 1.8 u.a for Cs and F, respectively, while for, Ca and Sr they were chosen to be 2.0, 2.2 u.a, respectively.

The maximum $l$ quantum number for the wavefunction expansions inside the spheres was confined to $l_{\max} = 10$. The plane wave cutoff and the number of $k$-points were both varied to ensure total energy convergence. The integrals over the Brillouin zone (BR) are performed up to 56 $k$-points for the structural properties and 451 $k$-points for the electronic and optical properties, in the irreducible Brillouin zone (IBZ), using the Monkhorst–Pack special $k$-points approach.[17] The self-consistent calculations are converged since the total energy of the system is stable within $10^{-5}$ Ryd.



## 3. Results and Discussions

### 3.1. *Structural properties*

The fluoroperovskite $CsMF_3$ (M = Ca, Sr) crystallizes in the cubic perovskite type structure with space group Pm3m (#221) and contains one molecule in its unit cell. The Cs atoms are positioned at the $(0; 0; 0)$ positions, the M atoms at $(0.5; 0.5; 0.5)$ and the three fluorine at $(0; 0.5; 0.5)$, $(0.5; 0; 0.5)$ and $(0.5; 0.5; 0)$. Our aim in this subsection is to calculate the total energy as a function of unit-cell volume around the equilibrium cell volume $V_0$. As a prototype the results obtained for $CsCaF_3$ are shown in Fig. 1. The calculated total energies versus volume are fitted with

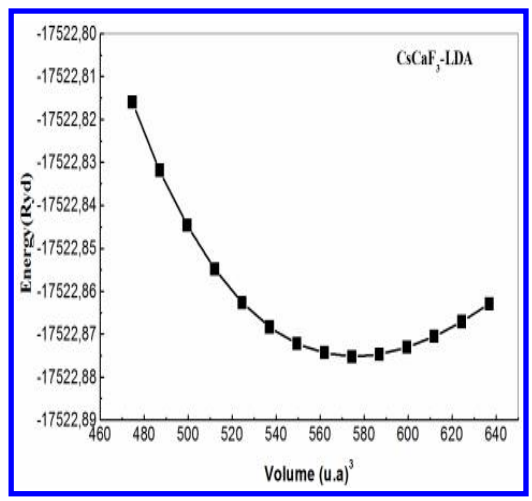


Fig. 1. Variation of total energy with unit cell volume for $CsCaF_3$ using LDA.

Table 1. Calculated lattice constant ($a$), bulk modulus ($B$), and its pressure derivative ($B'$) for fluoroperovskite compounds $CsCaF_3$ and $CsSrF_3$. Results are compared with the experiment and other theoretical works.

| | | Present work | | | |
|---|---|---|---|---|---|
| | | GGA | LDA | Experiment | Other theoretical works |
| $CsCaF_3$ | $a$ (Å) | 4.46 | 4.40 | 4.523[a] | 4.459[c,d] |
| | | | | 4.505[b] | 4.539[e] |
| | | | | | 4.4322[f] |
| | | | | | 4.403 (4.579)[g] |
| | | | | | 4.4144 (4.5771)[h] |
| | $B$ (GPa) | 62.93 | 67.19 | 44.147[c,d] | |
| | | | | | 67.008 (50.929)[g] |
| | | | | | 65.16 (46.53)[h] |
| | $B'$ | 4.43 | 4.55 | 4.598 (3.802)[g] | |
| | | | | | 4.66 (4.68)[h] |
| $CsSrF_3$ | $a$ (Å) | 4.70 | 4.64 | 4.75[a] | 4.414[c] |
| | | | | | 4.781[e] |
| | | | | | 4.6515 (4.8187)[h] |
| | $B$ (GPa) | 51.61 | 55.58 | | 26.33[c] |
| | | | | | 53.10 (38.97)[h] |
| | $B'$ | 4.58 | 4.52 | | |

[a]Ref. 19.
[b]Ref. 20.
[c]Ref. 21.
[d]Ref. 22.
[e]Ref. 23.
[f]Ref. 25.
[g]Ref. 26, LDA (GGA).
[h]Ref. 27, LDA (GGA).



the Murnaghan equation of state (EOS)[18] to obtain an analytical interpolation of our computed points from which we determine the ground state properties such as the equilibrium lattice constant $a_0$, the bulk modulus $B_0$ and its pressure derivative $B'$. The calculated equilibrium parameters ($a_0$, $B$ and $B'$) are listed in Table 1 which also contains experimental data[19,20] and previous theoretical results obtained by using the *ab initio* perturbed-ion model (*ai*PI),[21,22] the empirical model[23] and the support vector regression model (SVR models were developed for holdout and self-consistency tests),[24] the Gordon–Kim pair potentials in the quasi-harmonic approximation,[25] the FP-LAPW to the DFT[26] and the pseudo potential plane wave method based on the DFT.[27] It is clearly seen that for both compounds the GGA slightly overestimates the lattice parameters and underestimates the bulk modulus while the LDA slightly underestimates the lattice parameters and overestimates the bulk modulus, these findings are consistent with the general trend of these approximations. It is also observed that a larger lattice constant leads to a smaller bulk modulus. This result can be explained by considering the radius of M cations (Ca and Sr). The lattice constant increases when replacing Ca with the larger Sr ion, so for compounds after substitution, the lattice constant should be in-

creased if the atom in the cell is substituted by a larger atom, and decreased if by a smaller one.

### 3.2. *Electronic properties*

The calculated LDA-band structure for $CsCaF_3$ and $CsSrF_3$ compounds along some high symmetry directions in the first BZ at equilibrium volume are given in Fig. 2. The zero energy is chosen to coincide with the top of the valence band. In view of this figure, it is clear that the overall band profile is predicted to be the same for both compounds. In our calculations, a nine valence bands at Γ point are the threefold degenerate levels ($\Gamma_{15}$, $\Gamma_{25}$ and $\Gamma_{15}$) separated by energies of 0.052 eV ($\Gamma_{15} - \Gamma_{25}$) and 0.49 eV ($\Gamma_{25} - \Gamma_{15}$) in $CsCaF_3$; 0.17 eV and 0.36 eV in $CsSrF_3$. The split

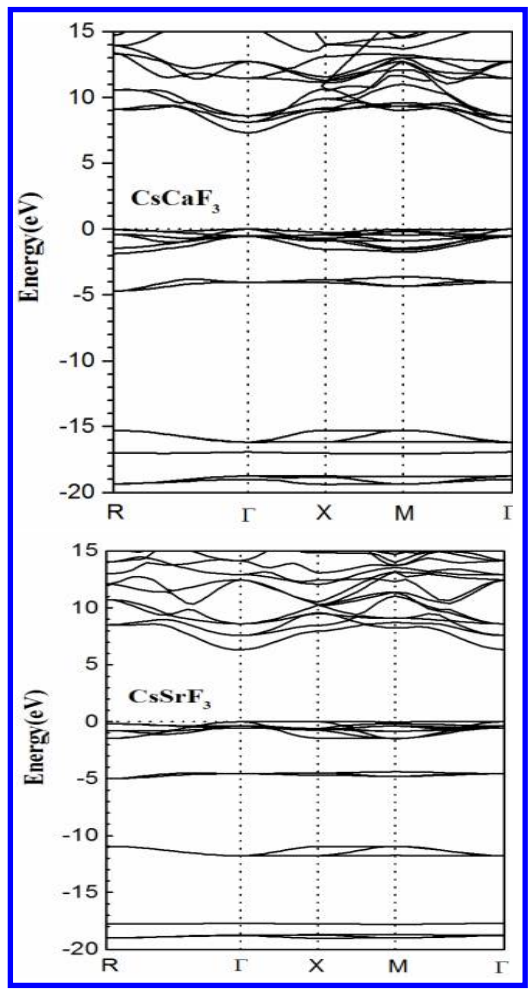


Fig. 2. Calculated electronic band structure of $CsCaF_3$ and $CsSrF_3$ using the LDA approximation.

of these levels is produced by the crystalline field and the electrostatic interactions between mainly three F atoms. The results of our calculations using LDA and GGA approximation show that the overall band profiles are in fairly good agreement with the FP-LAPW calculations[26] for the valence and conduction band configuration. For both compounds the conduction band minimum (CBM) and the valence band maximum (VBM) are located at the Γ point in BZ, resulting in a direct band gap (Γ − Γ). Our results on the nature of band gap of the studied compounds are in disagreement with those obtained by using the plane wave pseudo potential (PW-PP) and the linear combination of atomic orbitals (LCAO) methods.[27,28] These later determine the (VBM) at the *R*-point and the (CBM) at the Γ point, predicting these compounds as indirect band gap materials (*R*−Γ). The LDA (GGA) computed insulating Γ − Γ band gap are found to be equal to 7.33 (7.05) eV and 6.32 (6.17) eV for $CsCaF_3$ and $CsSrF_3$, respectively. Some calculated direct band gaps as well as the upper valence bandwidth values for the investigated compounds within the GGA and LDA approximations are listed in Table 2. The energy band gap decreases as traversed from Ca to Sr elements due to the shift that occurs for the conducting band of Cs *d*-band toward lower energies. The computed direct band gap values of $CsCaF_3$ compound are in excellent agreement with the theoretical ones quoted in Refs. 26 and 29, but they are relatively smaller than those obtained by using the LCAO method.[28] To the best of our knowledge no experimental values of the band gaps for the herein studied compounds are available for purpose comparison. Future experimental measurements will however testify all previous calculated results. The computed band gap values of $CsCaF_3$ and $CaSrF_3$ are nearly equal to those of $KXF_3$ ($X$ = Mg and Zn),[30–33] larger than those of $CsXF_3$ ($X$ = Hg, Cd and Pb),[27,28,34] $BaXF_3$ ($X$ = K and Rb)[35] and other oxide perovskites,[36–40] meaning that despite the identical crystal structure, compounds with this structure exhibit quite different electronic properties. It is well-known that quasiparticle GW remains a successful approximation for the calculation of the excitation energies, yielding an energy band

Table 2. Calculated energy gaps at high symmetry points in $CsCaF_3$ and $CsSrF_3$ compounds (energies are in eV). Results are compared with previous theoretical works.

| | Γ − Γ | $X - X$ | $R - R$ | $M - M$ | Upper bandwidth |
|---|---|---|---|---|---|
| $CsCaF_3$ | | | | | |
| LDA | 7.33 | 9.19 | 9.13 | 9.06 | 1.87 |
| GGA | 7.05 | 8.95 | 8.88 | 8.78 | 1.80 |
| Others | 7.274 (7.031)[a] | 9.197 (8.866)[a] | 9.143 (8.874)[a] | 8.973 (8.665)[g] | 1.919 (1.732)[g] |
| | 6.9[b] | | | | 2.4[b] |
| | 9.824[c] | 12.473[c] | 13.33[c] | 12.659[c] | |
| $CsSrF_3$ | | | | | |
| LDA | 6.32 | 7.96 | 8.68 | 8.25 | 1.48 |
| GGA | 6.17 | 7.84 | 8.48 | 8.11 | 1.38 |

[a]Ref. 26, LDA (GGA).
[b]Ref. 29.
[c]Ref. 28.

gap value close to the measured one,[41,42] while the density functional formalism with LDA and GGA is limited in its validity (see. Ref. 43) since the band structure derived from it usually yields smaller fundamental band gap of semiconductors and insulators when compared with experiment.[44] This underestimation is due to the wrong interpretation of the true unoccupied states of the system with the corresponding Khon–Sham states of DFT, meaning that these compounds may have a larger band gaps than those computed in the present work.

To further elucidate the nature of the electronic band structure, we have also calculated the total and atomic site projected densities of states (DOS) of $CsCaF_3$ and $CsSrF_3$. These are displayed in Fig. 3 for the energy range from −20 eV to 15 eV. These figures reveal that there are five distinct structures in the density of electronic states separated by gaps. For both $CsCaF_3$ and $CsSrF_3$ compounds, the upper valence bands ranging from −2.0 eV to Fermi level is mainly originating from Fluorine "2$p$" states. The band situated at around −5 eV for both compounds are essentially dominated by Cesium "5$p$" states. The Fluorine "2$s$" states with a few contribution from Calcium "3$p$" and Strontium "4$p$" states are located at around −19.54 eV and −19.1 eV in $CsCaF_3$ and $CsSrF_3$, respectively. The total DOS of

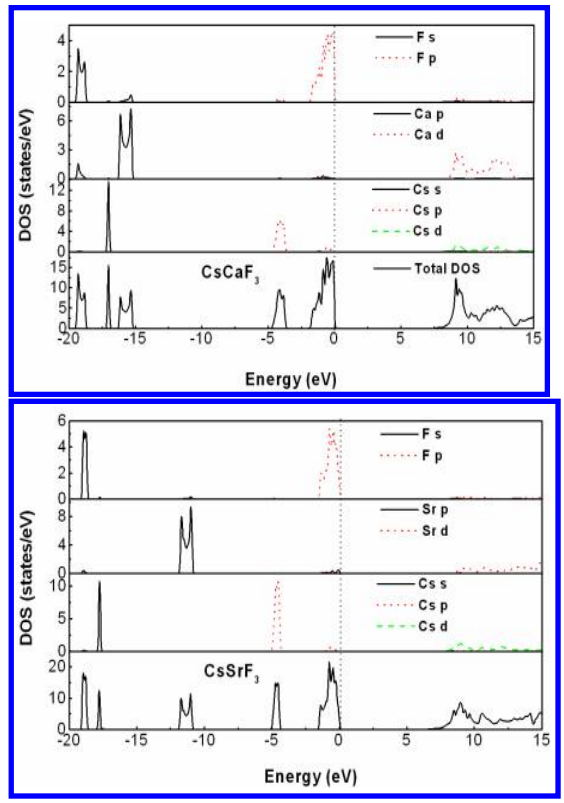


Fig. 3. Calculated partial (PDOS) and total density (TDOS) of states for the $CsCaF_3$ and $CsSrF_3$ compounds.

these compounds shows narrower peak situated at around −17.2 eV for $CsCaF_3$ and −17.9 eV for $CsSrF_3$ which correspond to a flat band formed by Cesium "6*s*" states. In both compounds, the peak around −16.4 eV and −11.9 eV represents a contribution of Calcium "3*p*" and Strontium "4*p*" states with a mixture from Fluorine "2*s*" states. The bottom of the conduction bands is dominated by Calcium and Strontium "*d*" states hybridized with Cesium "4*d*" and Fluorine "2*p*" states. All of these states are distributed in a wide energy range from 7.5 to 13.0 eV.

In order to understand the bonding nature in these compounds, the charge distribution is examined. Contours maps of the charge density along the [1 1 0] direction in $CsCaF_3$ and $CsSrF_3$ are shown in Fig. 4. Following this figure it is seen that $CsCaF_3$ and $CsSrF_3$ compounds are both found to have similar charge densities. Therefore, the bonds between cesium and fluorine atoms seem to have an ionic character. Moreover, the charge transfer occurs mainly from the other



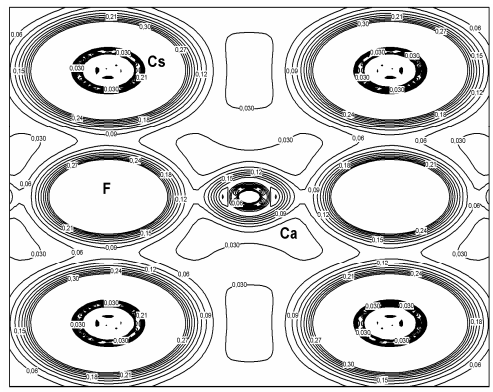


(a)

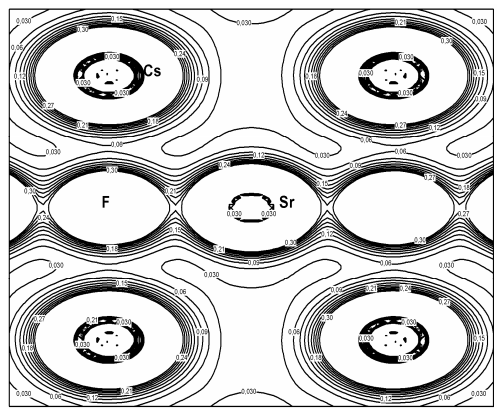


(b)

Fig. 4. Calculated charge density along the [1 1 0] direction in $CsCaF_3$ (a) and $CsSrF_3$ (b) at the predicted equilibrium lattice constant.

atomic species towards the fluorine atoms. Furthermore, the Sr–F bond is more ionic than the Ca–F bond, i.e., Ca–F bonds have stronger hybridization than Sr–F ones. Indeed, when moving down in a column for a group, the size of atoms increases. The electrons in larger atoms are not held as strongly as those in smaller ones. Hence, electronegativity decreases. Additionally, when a chemical bond is formed with another element and the difference of electronegativity is large, the bond tends to be more ionic.[45] Our results show that $CsCaF_3$ and $CsSrF_3$ are both ionic compounds.

### 3.3. *Optical properties*



The optical properties of matter can be described from the knowledge of the complex dielectric function $\varepsilon(\omega) = \varepsilon_1(\omega) + i\varepsilon_2(\omega)$.[46–49] $\varepsilon_1(\omega)$ and $\varepsilon_2(\omega)$ are the real and imaginary components of the dielectric function, respectively. The imaginary part $\varepsilon_2(\omega)$ is directly related to the electronic band structure and it can be computed by summing up all possible transitions from the occupied to the unoccupied states, taking into account the appropriate transition dipole matrix elements using the following expression[50–53]:

$$\varepsilon_2(\omega) = \frac{e^2\hbar}{\pi m^2\omega^2} \sum_{v,c} \int_{\mathrm{BZ}} |M_{cv}(k)|^2 \delta[\omega_{cv}(k) - \omega] d^3k \,. \tag{1}$$

The integral is over the first BZ. $M_{cv}(k) = \langle u_{ck}|\boldsymbol{\delta}\cdot\nabla|u_{vk}\rangle$, where $\boldsymbol{\delta}$ is the potential vector defining the electric field, are the dipole matrix elements for direct transitions between valence band $u_{vk}(r)$ and conduction band $u_{ck}(r)$ states, and the energy $\hbar\omega_{cv}(k) = E_{ck} - E_{vk}$ is the corresponding transition energy.

The real part $\varepsilon_1(\omega)$ can be derived from the imaginary part using the familiar Kramers–Kronig transformation[54]:

$$\varepsilon_1(\omega) = 1 + \frac{2}{\pi} P \int_0^\infty \frac{\omega' \varepsilon_2(\omega')}{\omega'^2 - \omega^2} d\omega' \,, \tag{2}$$

where, $P$ determines the principal value of the integral.

The knowledge of both real and imaginary parts of the dielectric function allows the calculation of important optical functions such as the refractive index $n(\omega)$ and extinction coefficient $k(\omega)$ using the following expressions[55–59]:

$$n(\omega) = \left[\frac{\varepsilon_1(\omega)}{2} + \frac{\sqrt{\varepsilon_1^2(\omega)+\varepsilon_2^2(\omega)}}{2}\right]^{1/2} , \tag{3}$$

$$k(\omega) = \left[-\frac{\varepsilon_1(\omega)}{2} + \frac{\sqrt{\varepsilon_1^2(\omega)+\varepsilon_2^2(\omega)}}{2}\right]^{1/2} . \tag{4}$$

Generally, there are two contributions to $\varepsilon(\omega)$, namely intraband and interband transitions. As a matter of fact the contribution from intraband transitions is crucial only for metals. The interband transitions can further be split into direct and

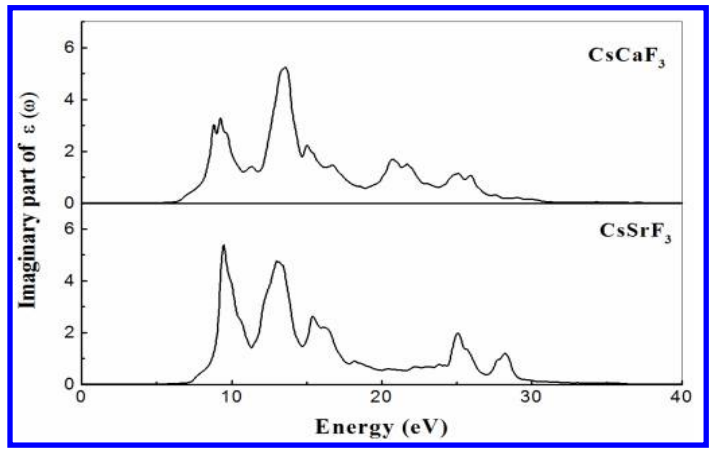


Fig. 5. Calculated imaginary part of the dielectric function of $CsCaF_3$ and $CsSrF_3$ compounds.



indirect transitions. Here, we neglect the indirect interband transitions which involve scattering of phonons and are assumed to give only a small contributions to $\varepsilon(\omega)$. Figure 5 shows the variation of the imaginary part of the dielectric function $\varepsilon_2(\omega)$ spectrum for a radiation up to 40 eV within LDA approximation for $CsCaF_3$ and $CsSrF_3$. As it can be seen that the optical spectra does not vary greatly from $CsCaF_3$ to $CsSrF_3$. This is attributed to the fact that the conduction bands features and the symmetries of the wavefunctions, which dictate the selection rules and are fully reflected in the matrix moment elements, are somewhat similar. Our calculated $\varepsilon_2(\omega)$ spectra show that the first critical points (threshold energy) of the dielectric function occur at about 6.42 eV and 6.25 eV for $CsCaF_3$ and $CsSrF_3$, respectively. These points are the direct optical transitions between the top of the valence band and the bottom of the conduction band at the $\Gamma$ point. This is known as the fundamental absorption edge. The first critical points are followed by five peaks in both compounds. These peaks are positioned at 9.48, 13.02, 15.38, 25.07 and 28.23 eV for $CsCaF_3$ and at 9.24, 13.54, 15.00, 20.70 and 25.01 eV for $CsSrF_3$. The pseudo potential plane wave calculations determine the threshold energy and the first peak at 6.6 eV and 9.21 eV for $CsCaF_3$ and at 6.03 eV and 9.03 eV for $CsSrF_3$, showing that our calculated optical spectra are slightly shifted with an enhanced energy. The reason lies on the slight deference in the band structures.

The results for the dispersive part of the dielectric function $\varepsilon_1(\omega)$ for the compounds under investigation are given in Fig. 6. The main features in these curves are: two peaks around 9.0 eV and 12.0 eV, a rather steep decrease between 12.5 eV and 13.5 eV eV for $CsCaF_3$ and $CsSrF_3$, respectively. After which $\varepsilon_1(\omega)$ becomes negative, minimum, followed by a slow increase towards zero at high energies. For the real dielectric function, the most important quantity is the zero frequency limit $\varepsilon_1(0)$, since it gives the static dielectric constant in the zero frequency limit, which has the value of 2.56 a.u and 2.45 a.u in $CsCaF_3$ and $CsSrF_3$, respectively. The extinction coefficient $k(\omega)$ and the refractive index $n(\omega)$ have been calculated. The

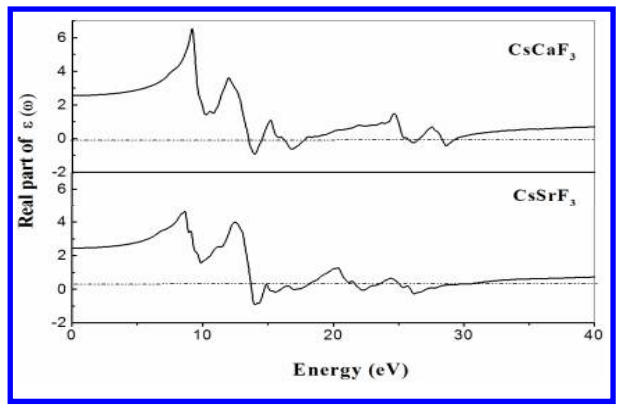


Fig. 6. Calculated real part of the dielectric function of $CsCaF_3$ and $CsSrF_3$ compounds.

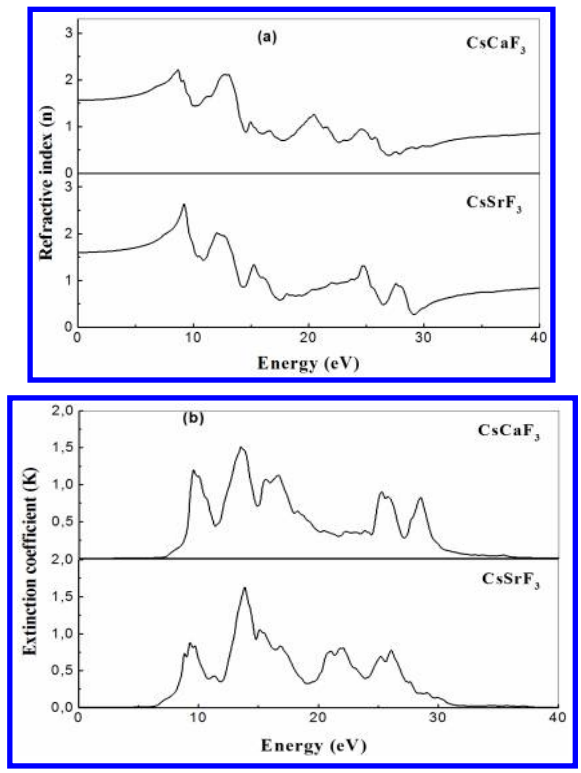


Fig. 7. Calculated refractive index (a) and extinction coefficient (b) of $CsCaF_3$ and $CsSrF_3$ compounds.

local maxima of the extinction coefficient $k(\omega)$ correspond to the zero of $\varepsilon_1(\omega)$. From Fig. 7, we note that in these compounds the extinction coefficient and the refractive index have resonance in the low energy region. The static value for the refractive index, which represents the important quantity, is 1.60 a.u for $CsCaF_3$

and 1.56 a.u for $CsSrF_3$. On the whole, the obtained refractive index spectra show that the refractive index is significant only up to 25.70 eV in $CsCaF_3$ and 28.10 eV in $CsSrF_3$. Beyond these energies, the refractive index drops sharply.

## 4. Conclusions

The structural, electronic and optical properties of $CsCaF_3$ and $CsSrF_3$ compounds are studied using the FP-LAPW method based on the DFT with both the LDA and GGA for the exchange-correlation functional. Structural parameters are found to compare well with the available experimental and theoretical data. The electronic structure calculations showed that $CsCaF_3$ and $CsSrF_3$ compounds are both ionic and exhibits a wide direct band gap at the Γ point in the BZ. Corresponding densities of states are presented and the major structures in them are identified. The origin of the different optical properties between the two materials has been discussed. The real and imaginary parts of dielectric function and hence the optical constants such as refractive index and extinction coefficient are calculated.



## Acknowledgments

R. Khenata and S. Bin-Omran acknowledge the financial support by the Deanship of Scientific Research at King Saud University for funding the work through the research group project N0 RPG-VPP-088. For author H. Khachai this work has been supported by the Algerian national research projects PNR (No: 8/U310/4153).

## References

1. http://research.chemistry.ohio-state.edu/woodward/.
2. B. Ghebouli *et al.*, *Solid State Commun.* **150**, 1896 (2010).
3. M. W. Lufaso and P. M. Woodward, *Acta Cryst. B* **57**, 725 (2001).
4. G. Horsch and H. J. Paus, *Opt. Commun.* **60**, 69 (1986).
5. R. Hua *et al.*, *J. Sol. State Chem.* **175**, 284 (2003).
6. A. V. Chadwick *et al.*, *Solid State Ion.* **9—10**, 555 (1983).
7. P. Berastegui, S. Hull and S.-G. Eriksson, *J. Phys.: Condens. Matter* **13**, 5077 (2001).
8. J. Julliard and J. Nouet, *Rev. Phys. Appl.* **10**, 325 (1975).
9. R. R. Daniels *et al.*, *Phys. Rev. B* **27**, 3878 (1983).
10. P. Blaha *et al.*, *Comput. Phys. Commun.* **59**, 399 (1990).
11. P. Blaha *et al.*, WIEN2K, *An Augmented Plane Wave Plus Local Orbitals Program for Calculating Crystal Properties* (Vienna University of Technology, Austria, 2001).
12. P. Hohenberg and W. Kohn, *Phys. Rev. B* **136**, 864 (1964).
13. S. Gao, *Comput. Phys. Commun.* **153**, 190 (2003).
14. K. Schwarz, *J. Solid State Chem.* **176**, 319 (2003).
15. J. P. Perdew and Y. Wang, *Phys. Rev. B* **45**, 13244 (1992).
16. J. P. Perdew, K. Burke and M. Ernzerlof, *Phys. Rev. Lett.* **77**, 3865 (1996).
17. H. J. Monkhorst and J. D. Pack, *Phys. Rev. B* **13**, 5188 (1976).
18. F. D. Murnaghan, *Proc. Natl. Acad. Sci. USA* **3**, 244 (1944).
19. O. Muller and R. Roy, *The Major Ternary Structural Familles* (Springer-Verlag, New York, 1974), pp. 76–78.

20. C. Ridou *et al.*, *J. Phys. C* **17**, 1001 (1984).
21. V. Luana, A. Costales and A. M. Pendas, *Phys. Rev. B* **55**, 4285 (1997).
22. V. Luana *et al.*, *Solid State Commun.* **104**, 47 (1997).
23. L. Q. Jiang *et al.*. *J. Phys. Chem. Solids* **67**, 1531 (2006).
24. A. Majid and Y. S. Lee, *Int. J. Adv. Inform. Sci. Serv. Sci.* **3**, 118 (2010).
25. L. L. Boyer, *J. Phys. C: Solid State Phys.* **17**, 1825 (1984).
26. A. Meziani and H. Belkhir, *Comput. Mater. Sci.* **61**, 67 (2012).
27. B. Ghebouli *et al.*, *Solid State Sci.* **14**, 903 (2012).
28. C.-G. Ma and M. G. Brik, *Comput. Mater. Sci.* **58**, 101 (2012).
29. Y. Chornodolskeyy *et al.*, *J. Phys. Stud.* **11**, 421 (2007).
30. T. Seddik *et al.*, *Appl. Phys. A* **106**, 645 (2012).
31. M. Sahnoun *et al.*, *Mater. Chem. Phys.* **91**, 185 (2005).
32. S. Cui *et al.*, *J. Alloys Comp.* **484**, 597 (2009).
33. G. Vaitheeswaran *et al.*, *Phys. Rev. B* **76**, 014107 (2007).
34. G. Vaitheeswaran *et al.*, *Phys. Rev. B* **81**, 075105 (2010).
35. A. A. Mubarak and A. A. Mousa, *Comput. Mater. Sci.* **59**, 6 (2012).
36. D. Cherrad *et al.*, *Physica B* **406**, 2714 (2011).
37. D. Cherrad *et al.*, *Physica B* **405**, 3862 (2010).
38. A. Bouhemadou, F. Djabi and R. Khenata, *Phys. Lett. A*, **372**, 4527 (2008).
39. A. Bouhemadou, F. Djabi and R. Khenata, *Solid State Sci.* **11**, 556 (2009).
40. R. Khenata *et al.*, *Solid State Commun.* **136**, 120 (2005).
41. M. S. Hybertsen and S. G. Louie, *Phys. Rev. Lett.* **55**, 1418 (1985).
42. M. S. Hybertsen and S. G. Louie, *Phys. Rev. B* **34**, 5390 (1986).
43. G. Onida, L. Reining and A. Rubio, *Rev. Mod. Phys.* **74**(2), 601 (2002).
44. P. Dufek, P. Blaha and K. Schwarz, *Phys. Rev. B* **50**, 7279 (1994).
45. D. D. Ebbing and M. S. Wrighton, *General Chemistry* (Houghton Mifflin, Boston, 1984).
46. J. S. Tell, *Phys. Rev.* **104**, 1760 (1956).
47. L. D. Landau and E. M. Lifshitz, *Electrodynamics in Continuous Media* (Pergamon Press, Oxford, 1960).
48. H. A. Kramers, *Collected Science Papers* (North Holland, Amsterdam, 1956), p. 333.
49. R. De L. Kron, *J. Opt. Soc. Am.* **12**, 547 (1926).
50. F. Bassani and G. P. Parravicini, *Electronic States and Optical Transitions in Solids* (Pergamon Press, Oxford, 1973).
51. P. Puschnig and C. Ambrosch-Draxl, *Phys. Rev. B* **66**, 165105 (2002).
52. C. Ambrosch-Draxl and J. O. Sofo, *Comput. Phys. Commun.* **175**, 1 (2006).
53. S. Sharma *et al.*, *Phys. Rev. B* **60**, 8610 (1999).
54. P. Y. Yu and M. Cardona, *Fundamentals of Semiconductors* (Springer-Verlag, Berlin, 1996), p. 233.
55. A. Delin *et al.*, *Phys. Rev. B* **54**, 1673 (1996).
56. P. Ravindran *et al.*, *Phys. Rev. B* **59**, 1776 (1999).
57. P. Ravindran *et al.*, *Phys. Rev. B* **59**, 15680 (1999).
58. M. M. Fox, *Optical Properties of Solids* (Oxford University Press, New York, 2001).
59. M. Dressel, *Proc. Natl. Acad. Sci. USA* **30**, 244 (1944).